Amirmasoud Mohtasebi[1] / Peter Kruse[1]

Chemical sensors based on surface charge transfer

[1] Department of Chemistry and Chemical Biology, McMaster University, 1280 Main Street West, Hamilton, Ontario, L8S 4M1, Canada, E-mail: pkruse@mcmaster.ca

Abstract:
The focus of this review is an introduction to chemiresistive chemical sensors. The general concept of chemical sensors is briefly introduced, followed by different architectures of chemiresistive sensors and relevant materials. For several of the most common systems, the fabrication of the active materials used in such sensors and their properties are discussed. Furthermore, the sensing mechanism, advantages, and limitations of each group of chemiresistive sensors are briefly elaborated. Compared to electrochemical sensors, chemiresistive sensors have the key advantage of a simpler geometry, eliminating the need for a reference electrode. The performance of bulk chemiresistors can be improved upon by using freestanding ultra-thin films (nanomaterials) or field effect geometries. Both of those concepts have also been combined in a gateless geometry, where charge transport though a percolation network of nanomaterials is modulated via adsorbate doping.

Keywords: chemical sensor, chemiresistor, CHEMFET, gateless FET, surface doping

DOI: 10.1515/psr-2017-0133

1 Chemical sensors

A chemical sensor is a device which can measure analytical parameters and convert the chemical data into a measurable signal [1]. Each chemical sensor consists of two functionally distinct parts, a detector and a transducer. The detector (receptor) transforms the chemical information into a form of energy while the transducer transforms this energy to a measurable signal [2]. The transduction mechanism of chemical sensors is a criterion which can be used for their categorization. Based on this criterion, the most common groups of chemical sensors are optical sensors, electrochemical sensors, and electrical sensors. In optical sensors, the change in the optical properties of a reagent upon interaction with an analyte is measured. Some commonly measured optical properties are absorption, fluorescence, light scattering, and decay time. Indicator papers are a very simple form of optical sensors in which a reagent has been covalently immobilized on a paper substrate. While indicator papers are cheap, quick, and easy to use, they are not very accurate, and they cannot be used for continuous, automated, or remote monitoring. The advances in optoelectronic device fabrication in recent years have aided in the development of high-quality light sources, photodetectors, and fiber optics which can be used to develop inexpensive and reliable optical sensors. These achievements have made optical sensors a popular choice for various applications from water quality monitoring to biomedical applications. However, optical access to the analyte may be restricted by turbidity, deposits, or other interferences, adding to the complexity of such sensors.

Another widely used group of chemical sensors are electrochemical sensors, most commonly used in pH measurement in which the activity of the hydronium ions is measured [1, 2]. In the simplest case, electrochemical sensors consist of two conductive electrodes and an electrolyte. However, a third electrode is normally required as a reference electrode to maintain accuracy and precision of the measurements. Electrochemical sensors are designed based on various electrochemical techniques such as voltammetry, amperometry, potentiometry, and impedometry. The two former methods are most often used in chemical sensors. In voltammetric measurements, the potential applied to an electrode is linearly ramped to be more negative and followed by ramping back to a more positive potential while during this cycle the current is measured. In forward scan, the reduction of an analyte at any of the applied potentials is monitored. Once the applied potential is equal to the reduction potential of the analyte the measured current increases. This is followed by the reduction of the measured current as a result of the depletion of the analyte in the vicinity of the electrode. In the reverse scan, at a certain potential the analyte will be reoxidized to its initial form. This will appear as a peak with a reverse sign as the reduction peak. Theoretically, for a reversible process the difference between the reduction and oxidation peaks is about 59 mV [3, 4]. In amperometric measurements, a constant potential is applied and

Peter Kruse is the corresponding author.

the change in current as a function of time is monitored. The value for this potential can be determined from the voltammogram of the analyte of interest [2].

Chemical sensors can also operate based on electrical transduction. These sensors are distinct from electrochemical sensors because they do not rely on maintaining precise electrode potentials, thus removing the requirement for a reference electrode in liquids as well as in the gas phase. Chemiresistive sensors are the main group of sensors based on electrical transduction. In these sensors, the changes in the conductivity of an active layer are used to detect the presence of an analyte. Various types of interactions between the active material and the analyte can lead to a change in the conductivity of the active layer. For example, the analyte can cause oxidation or reduction of the active layer, or the analyte can undergo charge transfer with the active layer through processes such as surface doping [5]. More sophisticated sensors based on electrical transduction are based on the field effect transistor (FET) architecture. Therefore, this group of sensors is called chemical FET (CHEMFET). Most commonly in CHEMFETs, the interaction of the analyte with the gate electrode is used to modulate the charge transport in the conductive channel [6]. However, the use of the direct interaction of the analyte with the conductive channel to modulate the charge transport has also been reported. The former architecture is simpler than the traditional CHEMFET as the dielectric layer and the gate electrode have been removed [7]. The summary of chemical sensors based on their sensing principle can be found in Table 1.

Table 1: Summary of different chemical sensors based on their sensing principle.

Sensor Class	Sensing Principle	References
Optical	Colorimetric	[8]
	Absorptivity	[9]
	Chemiluminescence	[10]
Electrochemical	Amperometric	[11]
	Voltammetric	[4, 12, 13]
	Electrochemical gas sensor	[14]
	Chemiresistive	[5, 41, 107]
Electrical	CHEMFET	[6]
	Ion Selective FET	[6, 96]
	Work Function FET	[15]
	OFET	[96, 99, 100]
	Gateless FET	[7, 101]

2 Chemiresistive sensors

2.1 Metal oxide thin film chemiresistive sensors

Some of the earliest work on chemical sensors based on electrical transduction has been reported for chemiresistive sensors [16, 17]. These devices operate on the principle that the adsorption of chemical species onto the surface of a conducting or semiconducting material leads to changes in the electrical properties of the substrate, mainly its electrical conductivity. The conductive substrate can be simply attached to conductive electrical leads connected to a source measurement unit [17]. More sophisticated contact geometries include four-point electrical contacts or interdigitated electrodes [18]. The chemical species can interact with the sensing film through various pathways such as physisorption, chemisorption, catalytic reactions, reactions at grain boundaries, and bulk reactions. The change in the electrical properties of the sensing material by the adsorbed chemical species on its surface can be caused by different processes such as oxidation/reduction of the surface or changes in the surface work function [18]. Table 2 shows the most common categories of sensitive materials used in chemiresistive sensors.

Table 2: Common sensitive layers used in chemiresistive sensors.

Type of Sensitive Layer	Examples of Sensitive Materials	References
Metal oxides, semiconductors	SnO_2, TiO_2, Co_3O_4, In_2O_3	[18–21]
Conductive Polymers	Polyaniline, polypyrrole, polycarbazole	[5, 22, 23, 41, 51]
Nanocarbons	Carbon nanotubes, graphene, pencil lead	[24, 25, 55, 57, 101]

Early work on chemiresistive sensors was performed using thin or thick oxide films such as tin oxide [18]. It was shown that the adsorption of oxygen molecules on this surface leads to the formation of O_2^- and O^-. Since the tin oxide is an intrinsic n-doped semiconductor, the flow of electrons from the metal oxide film to these species leads to a decrease in its electrical conductivity. Upon exposure of this surface to a reducing gas (e. g. H_2, NH_3, CO) the electron transfer from the adsorbed gases to the metal oxide leads to an increase in the electrical conductivity of the substrate while the adsorption of an oxidizing gas such as NO_2 leads to the opposite response. In the latter situation, the direction of the charge transfer is opposite, causing the formation of NO_2^- and thus reduction in the conductivity of the metal oxide [16, 17, 26]. Mechanistic studies have found that in addition to increasing the surface area to volume ratio, the sensor performance can be enhanced by increasing the surface defect density of the metal oxide, and by careful tuning of the band structures and potential barriers at junctions within the device [27]. This emphasizes the role of the surface defects in the molecular recognition process. The most common metal oxides used in chemiresistive sensors are summarized in Table 3.

Table 3: Examples of some of the common metal oxides used in chemiresistive sensors and some of the analytes that have been detected by them.

Sensitive layer	Analyte(s)	Operating temperature, response time, tested concentrations	Reference
Fe_2O_3	Gas: Humidity	r.t., 10 sec, 20 ... 90 %	[28]
In_2O_3	Gas: CO, H_2	>200 °C, 1 ... 100 sec, 0.1 ... 0.5 %	[21]
NiO, WO_3, ZnO, SnO_2, Nb_2O_5	Gas: CO, NO_2	100 ... 400 °C, 5 ... 500 ppm CO, 0.2 ... 9 ppm NO_2	[29]
CaO @ ZnO	Gas: CO, NO_2	300 °C, 200 sec, 10 ... 200 ppm	[27]
Ga_2O_3	Gas: CO	500 °C, 200 ... 600 sec, 100 ppm	[30]
SnO_2	Gas: H_2S	r.t., 2 ... 13 sec, 10 ... 100 ppm	[31]
Co_3O_4	Gas: H_2S	325 °C, a few minutes, 1 ... 100 ppm	[20]
Fe_2O_3	Gas: Acetone, EtOH	350 °C, 10 ... 20 sec, 0.5 ... 50 ppm	[32]
ZnO	Gas: Acetone	r.t., 18 sec, 0.2 ... 100 ppm	[33]
TiO_2	Gas: Alcohols	r.t. to 250 °C, 2 ... 200 sec, 10 ... 1000 ppm	[35]

Since the sensing depends on chemisorption, the surface structure of the sensing film (grain boundaries, defects) plays a key role [18]. Figure 1 illustrates the schematic of the reaction of different gases with different surface sites available in a thin film sensor and the direction of the charge transfer for each surface–analyte interface. Although the sensing step in these sensors often can be performed at low temperatures (room temperature to 100 °C), the resetting step typically requires elevated temperatures in the range of 100–400 °C [18]. These high temperatures are essential for resetting the sensor as the thermal energy enhances the rate of the analyte desorption from the metal oxide surface [34]. However, the requirement for such step at high temperatures counts as the main drawback of these sensors and is the reason behind their limited application. In addition, the elevated temperatures can cause sintering of the sensing film which can alter its reaction sites essential for chemical sensing. Some of these reaction sites are point and bulk defects, and grain boundaries [18]. Not only do the surface defects play an essential role in the analyte recognition process [27], but they can also be tuned to enhance the sensor performance to a point where room temperature operation becomes possible [35].

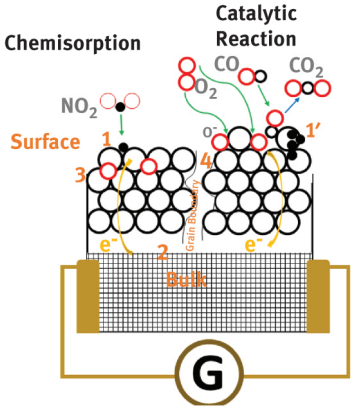

Figure 1: Schematic representation of the detection of gas molecules by an active layer in a chemiresistive sensor. Interaction of gas molecules leads to a change in the conductivity of the bulk and the surface of the active layer. Some of these reactions are from undoped (1) or doped surfaces (1´), from the bulk of the film (2), from the contacts (3), and from the grain boundaries (4).

The size of the grains of the polycrystalline metal oxide films has a significant effect on the sensitivity of these sensors. Generally, the reduction of the grain sizes to nanometer levels leads to an increase in sensitivity [36]. Another method to increase the gas sensitivity of the sensors is the use of suspended ultra-thin metal oxide films [37, 38]. These quasi two-dimensional films have a high surface area and thus most of the film can interact with the adsorbed gas analytes. Some of these films such as suspended porous tantalum oxide films can act like selective membranes. These oxide membranes can even further amplify the interaction with the gas analytes as the analyte can diffuse into the film [39]. In addition, this way the interaction of the sensing material with the substrate, which may affect the sensing process, is eliminated [5]. Although these films are thin, it has been shown that they can withstand flowrates as high as hundreds of milliliters per second and still sample the dilute gas analytes [40]. However, the use of two-dimensional metal oxide membranes has not lead to lower operational temperatures for chemiresistive sensors [39]. Figure 2 shows the schematic diagram of a gas dosing apparatus for sensor testing. The gas molecules flow from the gas source to the measurement chamber through Teflon tubes. The flow of the gas is controlled by mass flow controllers (MFC). The chamber is equipped with a heater to control the temperature of the system during the measurement and resting steps. The chamber is evacuated from interfering gasses by a vacuum pump. The sensor is placed inside a chamber and is electrically connected to the source measure unit (SMU). A quartz crystal microbalance (QCM) is placed close to the sensor to quantify the adsorption of the analyte gas on the surface. Both QCM and SMU are connected to a data acquisition system (DAQ, e. g. computer).

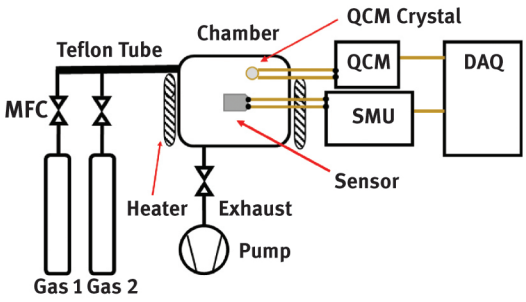

Figure 2: Schematic view of a gas dosing apparatus for sensor testing. The system consists of gas cylinders, mass flow controller (MFC), Teflon tubes, measurement chamber, quartz crystal microbalance (QCM), source measure unit (SMU), heater, data acquisition unit (DAQ), and exhaust system for evacuating the system.

2.2 Chemiresistive sensors based on intrinsically conducting polymers

Another group of materials which have been widely used for chemical sensing applications are intrinsically conducting polymers (ICP) and their oligomers. The common structure of ICPs consists of repeating units of small organic monomers. Figure 3 shows some of these polymers such as polyacetylene, polypyrrole, polythiophene, and polyaniline [17]. The conductivity of the ICPs originates from a conjugated system of alternating single and double bonds resulting in the formation of delocalized electronic states [5]. These polymers in their neutral forms are not electrically conductive but can be made conductive through n-doping or p-doping [41]. These processes lead to the generation of charge carriers on their backbone, which transform them into one-dimensional conductors [17]. Such changes in their conductivity upon interaction with various chemical species (redox, basic/acidic) can be utilized for sensing applications. The adsorbed gas molecules on such polymers can act as secondary dopants, exchanging charge carriers with polymers which can lead to the modulation of their electronic, optical, or magnetic properties [5].

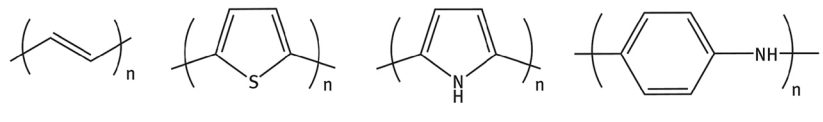

Figure 3: Molecular structure of four intrinsically conducting polymers in their undoped state.

Most of the chemical sensors that have been developed based on ICPs are gas sensors. In these sensors, the polymer can be used as either the selective sensing material or as an interconnect component. The latter application is not desired as the change in the electrical conductivity of the interconnect component can interfere with the main sensing process [5]. Therefore, the ICPs or other organic small molecules should only be used as the selective sensing material. The simplest and most common measurement configuration for chemical sensors based on ICPs is the chemiresistor with two electrical leads (Figure 4a). In this configuration, the polymer film is deposited between two electrodes (commonly Au) and a constant current or voltage is applied between them [41]. The gaseous analyte can interact with the ICP layer and act either as electron donor or electron acceptor. It will thus either enhance the degree of doping and increase the electrical conductivity of the film, or counteract the doping and decrease the electrical conductivity of the film [5]. Therefore, the most common way to report the response from chemiresistive sensors is in the form of $(R_1-R_0)/R_0$, where R_0 is the resistance of the system before the exposure to the analyte and R_1 is its resistance after exposure to the analyte [17]. This simple principle leads to the detection of the chemical species of interest present in the gas phase.

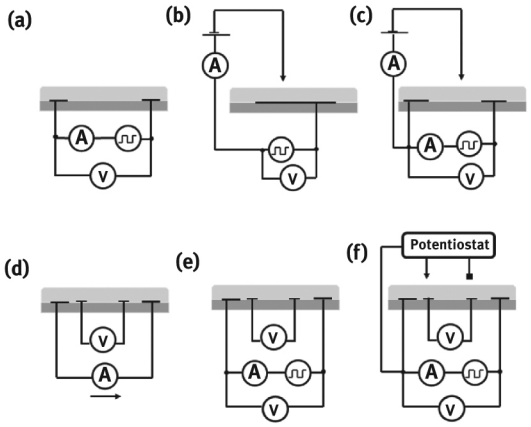

Figure 4: Common measurement configurations in chemiresistive sensors based on ICP selective layers. (a) Two-point measurement without fixation of the ICP layer potential, (b) typical set up used in electrochemical experiments, (c) Two-point measurement with fixation of the ICP layer potential, (d) Four-point technique, (e) Two- and Four- point measurement together without fixation of ICP potential, and (f) Two- and Four- point measurement together with fixation of ICP potential.

The drawback of this configuration is the drop of the potential at the metal-polymer contacts. A change in the electrical conductivity at this junction is attributed to the modulation of the Schottky barrier height which can be determined from the differences between the work functions of the polymer and the metal electrodes [5]. The materials choices for the metal electrode can also influence the nature of the contacts with the polymer film and result in a different magnitude of the response. It has been reported that the contact between gold and polyaniline (PANI) is ohmic while platinum (Pt) and PANI form a Schottky contact in the presence of hydrogen. The latter system showed a greater response (65 % increase in the resistance) to the presence of hydrogen gas in comparison to the former system (3 % decrease in the resistance). The absence of hydrogen in the chemical sensor based on Pt-PANI converts the contact between metal and polymer film back to ohmic [42]. One way to eliminate the contribution of the metal-polymer contact to the response of a chemical sensor is by use of a four-point measurement configuration (Figure 4d). However, this technique does not provide any information regarding the actual contact resistance, which is problematic in cases where the contact resistance is higher than the sensing response. The configuration in Figure 3(e) can be used to perform both two- and four-point measurements. It is also known as s24-configuration. This configuration enables the comparison of the delay time between the two- and four-point measurement signals which can provide information regarding the diffusion of the gas through the polymer layer.

Most of the sensing measurements using these configurations are performed by application of constant potential or constant current, which can itself cause irreversible or reversible changes in the polymer layer. This can be avoided by application of DC pulses or of AC (instead of DC). In addition, the probe power should be limited as it can lead to self-heating of the polymer layer [41]. Some other common sensing configurations involving two- and/or four- point configurations are shown in Figure 4(b, c, and f). Figure 4(b) shows the typical configuration which uses a conductive polymer layer in electrochemical systems. These configurations are based on organic field effect transistors in which the current between the source and the drain electrodes is regulated by the gate voltage [41]. The details of this type of chemical sensor will be further discussed along with CHEMFETs. In many chemical sensors based on conductive polymers, specifically in biosensors, the conductivity of the conductive polymer is low which makes it difficult to measure its conductivity between two electrodes. In such cases the conductivity between the conductive polymer layer and an electrode in solution is used for

measurement [41]. Figure 4(c) shows a somewhat similar configuration to the set up in Figure 4(b) with the difference that in the latter case the purpose of the external electrode is fixation of the polymer potential. This is useful if it is necessary to control the redox states of the polymer. This setup resembles the FET architecture as the external electrode can control the potential of the polymer layer and thus it was termed as electrochemical transistor setup [41]. Table 4 summarizes some of the most common ICPs used in chemiresistive sensors.

Table 4: Common ICPs used in chemiresistive sensors.

Sensitive layer	Analyte(s)	Operating temperature, Response time, tested concentrations	Reference
Polyaniline	Gas: CO	r.t., 100 sec, 1 ppm (in H_2)	[43]
	Gas: Humidity	r.t., 600 sec, 0 ... 100 %	[44]
	Aqueous: pH	r.t., pH 1 ... 6	[45]
Polypyrrole	Gas: NH_3	r.t., 10 sec, 0.1 ppb ... 2 ppm	[51]
	Gas: Humidity, alcohols, acetone	r.t., 400 sec	[46]
Polythiophene	Gas: Xylene Isomers	r.t. 400 ppm (selective for p-xylene)	[47]
Polycarbazole	Gas: H_2S	r.t., 600 sec, 1 ... 60 ppm	[23]
Poly(paraphenylene vinylene)	Gas: Ethyl acetate, n-propanol, methanol	r.t., 60 sec, saturated vapors	[48]
Poly(paraphenylene ethylene)	Gas: Menthol Enantiomers	r.t., 170 ... 1200 sec, 50 ... 300 ppm	[49]

Although chemiresistive sensors based on conductive polymers are simple, easy to fabricate, and can be prepared in various configurations, they have several drawbacks. The thickness of the organic film can greatly affect the response. Polymer films are porous and thus gas molecules of the analyte can diffuse through them [50]. The morphology of the polymer film (filament or dendritic, smooth, or compact) itself can also change the sensitivity of the device [51, 52]. Furthermore, the interface between the polymer film and the insulating substrate of the sensor itself can affect the electrical response. Last but not least, the copresence of different gases and moisture from the ambient environment can also interfere with the response to the analyte of interest [5, 53].

2.3 Chemiresistive sensors based on nanocarbons

Another group of materials that have been extensively incorporated into chemiresistive sensors are nanocarbons such as carbon nanotubes (CNTs) [54, 55], graphene [55–57], and even graphite or pencil lead [58]. Most of these materials are resistant to harsh chemical conditions and high temperatures [54, 58]. They are inexpensive or there is research underway for their mass production which will eventually reduce their production cost [59]. They are easy to fabricate on a wide range of substrates through various methods such as CVD [60], inkjet printing [61], or drop-casting [62]. All of this makes them suitable materials for sensing applications. They have been used for both gas sensing [54] and sensing in liquid phases [62].

CNTs are the most commonly used allotrope of carbon for chemiresistive sensors, mainly in the form of single-walled carbon nanotubes (SWCNTs). They are used as the sensing materials and often suspended over Au or Pt electrodes. One of the unique characteristics of CNTs is their high surface area (~1600 $m^2\ g^{-1}$) [54]. In addition, they have superb electrical properties such as carrier mobilities as high as ~10,000 $cm^2\ V^{-1}\ s^{-1}$ which is better than silicon and possible electrical current densities of up to ~ 4×10^9 A cm^{-2}, which is about a thousand times higher than copper [63]. CNTs can be chemically doped (p- or n- doped) by a wide range of chemical species [64–66]. The combination of these characteristics makes SWCNTs a better choice than metal oxides (e. g. SnO_2) or ICPs for sensing applications. In addition, in contrast to most metal oxide based sensors, they can operate at room temperature. The common sensing mechanism of chemical species by chemiresistive sensors based on CNTs is similar to what was described earlier for chemiresistive sensors based on ICPs/small molecules and metal oxides. The high surface area of CNTs allows for good interactions with the analyte molecules. The analyte molecules adsorb onto this surface and can transfer charge to or from the CNTs and as a result change the charge polarity (doping) of CNTs [67]. This will lead to a change in the electrical conductivity of the CNTs and can be used for detection of analyte molecules [68].

A challenge in the fabrication of CNT devices is that CNTs usually are only available as mixes of tubes with very different mechanical and electrical properties. Even within each batch of synthesized CNTs, the diameters of the tubes are different. Since the bandgap of semiconducting CNTs has an inverse relationship with their

diameter, the bandgap of the tubes in each batch can vary over a broad range. For example, it was reported that the SWCNTs produced via laser-ablation can have diameters ranging from 11 to 16 Å which will lead to a variation in their bandgap from 0.95 to 0.65 eV [69]. These variations in diameter, bandgap, and their electronic type (metallic/semiconducting) can cause reproducibility issues for mass production of such sensors [54]. The presence of metallic CNTs is not usually a problem in chemiresistive sensors, but can cause shorts in the case of CNT-based FETs [54]. Fortunately, in recent years ways have been found to sort the as synthesized CNTs (especially SWCNTs) through various separation means in order to produce more homogenous batches of tubes [69].

An issue with the use of CNTs in electronic devices including chemiresistive sensors is the high contact resistance between the metal electrodes and the CNTs. Suspending CNTs over electrodes often causes unreliable contacts between the electrodes and CNTs. This issue can be circumvented by new techniques such as creating end-bonded contacts between CNTs and molybdenum to form molybdenum carbide [70]. Even though chemiresistive sensors based on CNTs are often more sensitive than those based on ICPs, both suffer from similar problems associated with the effects of interfering molecules present in uncontrolled environments such as ambient conditions. It is known that humidity, hydrogen bonding with oxygen defects, and direct water adsorption can greatly affect the baseline resistance of the sensor. Such cross sensitivity between interfering molecules and the analyte of interest makes the process of establishing a calibration curve for these sensors challenging [54].

Graphene is another popular nanocarbon for use in chemical sensors. Graphene is a flat monolayer of carbon atoms arranged in the form of a two-dimensional (2D) honeycomb lattice. Graphene is the basic building block of many carbon allotropes such as graphite (3D), CNTs (1D), and fullerenes (0D) [71]. The pioneering reports on the concept of graphene go back sixty years and relate to theoretical studies on the band structure of graphite [72–74]. For a long time, it was believed that the 2D crystals are thermodynamically unstable and as the lateral size increases would transform to a stable 3D structure [75]. The base of such argument was that the thermal fluctuations in low-dimensional crystals lead to the displacement of atoms over distances as large as their interatomic distances at any finite temperature. However, advances in fabrication and characterization of graphene demonstrated the possibility for 2D crystals to exist [76]. Graphene can be produced by several approaches such as mechanical exfoliation of graphite, chemical exfoliation of graphite, and epitaxial growth [71, 77, 78].

The s, p_x, and p_y orbitals of each carbon atom in a graphene sheet hybridize to form strong covalent sp^2 bonds leading to the chicken-wire-like arrangements. The p_z atomic orbitals of a large number of carbon atoms overlap with each other forming a filled π band (valance band, VB) and an empty π^* band (conduction band, CB). This means that three out of four valance electrons of each carbon atom form σ bonds while the fourth electron participates in π bonding [79, 80]. The superior electronic properties of graphene are mainly due to its high-quality 2D crystal structure. Although graphite is made of ABAB stacks of graphene sheets, their electronic structure is quite different. It is known that graphite is a semimetal while single layer graphene is known to be a zero-band gap semiconductor. The CB and VB of graphene are cone-shaped and meet each other at the Dirac point [81, 82]. By increasing the number of sheets in graphene, the crystal shows increasingly semimetallic behavior and for stacks of 11 or more sheets, the band overlap varies by less than 10 % from graphite [82]. Another unique electrical property of graphene is its high charge carrier mobility (as high as 20,000 cm^2/Vs for Si/SiO_2 supported graphene sheets under ambient conditions) [71].

Similar to CNTs, graphene can become both p-doped and n-doped through various means such as an applied electric field or by chemical dopants. The former method is based on the possibility to tune charge carriers between electrons and holes by changing the polarity of the gate voltage (V_g). This means when V_g is negative the Fermi level is below the Dirac point and the VB is full of holes and when the V_g is positive the Fermi level is above the Dirac point and the CB is filled with electrons [71]. The latter method (chemical doping) is similar to the doping of CNTs as described earlier. Therefore, it is not surprising that one of the first electronic devices developed based on graphene was a chemical sensor [83]. In fact, some of the most sensitive gas sensors ever developed are based on graphene which can detect adsorption/desorption of an individual gas molecule [56]. Upon adsorption of an individual gas molecule on graphene, the local carrier concentration in this substrate will change, which will appear as a step in the resistance. The reason behind the possibility to detect such a small change is the unique and extremely low-noise characteristic of graphene. Thus, the possibility of chemical doping of graphene is one of the bases of using this material in sensing devices [56]. In addition, graphene has a high surface area (>2000 m^2/g) which is an important aspect in sensing applications. It has an advantage over CNTs in that it can be prepared uniformly and in high quality with very few defect sites [84]. Graphene has been incorporated in both chemiresistors [85] and CHEMFETs [86]. These sensors have been used for both gas sensing and sensing in liquids [85, 86]. Graphene, similar to CNTs, suffers from high sensitivity to many interfering adsorbates (humidity, oxygen, etc.) that are present in liquids or in ambient conditions and decrease

the sensitivity of the device [85]. Table 5 summarizes some of the most common nanocarbon applications in chemiresistive sensors.

Table 5: Common nanocarbon materials used in chemiresistive sensors.

Sensitive layer	Analyte(s)	Operating temperature, response time, tested concentrations	Reference
CNTs	Gas: MEK, acetone, methanol, ethanol	r.t., 480 sec, saturated vapors	[87]
	Gas: Volatile organic carbons	r.t., 60 sec, 300 ... 2000 ppm	[88]
	Gas: Benzene, Toluene, Xylene	r.t., 50 sec, 0.5 ... 10 ppm	[89]
	Aqueous: Glycerol	r.t., 100 sec, 10 ... 50 %	[90]
	Aqueous: Free chlorine	r.t., 300 sec, 0.06 ... 60 ppm	[62]
	Aqueous: Free chlorine	r.t., 100 sec, 0.03 ... 8 ppm	[24]
Graphene	Gas: NH_3	r.t., 20 min, 15 ... 48 ppm	[91]
	Gas: NO_2, NH_3	r.t., 50 min, 0.1 ... 200 ppm	[92]
Reduced Graphene Oxide	Gas: NH_3	r.t., 30 sec, 100 ... 500 ppm	[93]
	Gas: NH_3	r.t., 350 ... 650 sec, 10 ... 50 ppm	[94]
Graphene Oxide	Gas: NO_2, NH_3, Cl_2	r.t., 200 sec, 0.5 ... 100 ppm	[95]
Graphite (Pencil)	Aqueous: Free chlorine	r.t., 50 sec, 0.1 ... 60 ppm	[101]
	Aqueous: Free chlorine	r.t., 300 sec, 0.06 ... 60 ppm	[102]

3 CHEMFET

Another configuration for chemical sensing is based on the field-effect geometry. The general idea behind these sensors is that the interaction of the analyte with the gate electrode affects the charge transport properties in the conductive channel of the FET. This is different from the general scheme of FETs in which the gate electrode is insulated from the surrounding environment (Insulated Gate FET, IGFET). Therefore, the gate electrode acts as the selective layer. The same technology which is used in the semiconductor industry for fabrication of FETs can be used for fabrication of these sensors. Therefore, they can be miniaturized since in CHEMFETs the signal does not depend on the size of the sensing area. However, the signal from these type of sensors is small and requires a high input impedance amplifier [6].

Traditionally, CHEMFETs are categorized according to two main configurations; ion-sensitive FET (ISFET, Figure 5a) and work function FET (WF-FET, Figure 5b). ISFET operation is based on the selective separation of ionic charge present in the analyte sample at its interface with the selective layer (e. g. ion selective membrane). Therefore, the interfacial potential follows the Nernst equation. Since the potential of a single electrode is not measurable, a second reference electrode is used to measure the potential difference between this electrode and the selective layer [6]. This design has been mostly used for pH measurements. Based on the analyte of interest, the selective layer of an ISFET can be fabricated from semiconducting inorganic or organic materials (e. g. ICPs) [96]. WF-FET operation resembles the working principle of Kelvin probes (vibrating capacitor) [97]. The schematic of this configuration is depicted in Figure 5(b). Since this configuration does not require the presence of an external electrode (unlike ISFET), they are suitable for miniaturization. It has been argued that the gate electrode in FETs is part of a capacitor consisting of the gate electrode (here selective layer), the dielectric layer, and the conductive channel (often Si in FETs). The two plates of this capacitor (selective layer and the channel) have different chemical potentials. Their connection leads to the equalization of their Fermi levels which results in formation of an electric field. Since in FETs the channel is sealed from the surrounding environment, its work function remains unchanged during the sensing events. Therefore, it can be used as a reference electrode [6]. The gate electrode in WF-FETs can be fabricated from ICPs [96]. The interaction of analyte molecules with this electrode leads to the charge transfer between them and the formation of donor/acceptor complexes [98]. The extent of this charge transfer depends on the electron affinity of the host material (selective layer) and the ability of the analyte species to donate electrons [6].

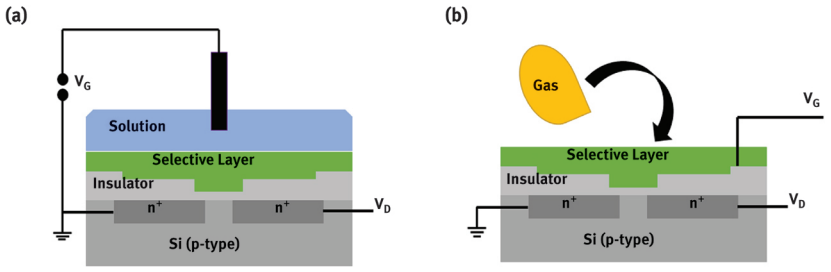

Figure 5: Schematic representation of two common architectures of CHEMFET. (a) ion sensitive (ISFET) sensor. (b) Work function sensor (WF-FET), in which no external reference electrode is required.

The gate electrode in FET sensors can be fabricated from ICPs. Thus, an extra layer of appropriate ICP is fabricated on the dielectric layer and will interact with the measurement environment [96]. This organic semiconductor layer can be further functionalized with biological receptors for biosensing purposes. The common ICPs used in such sensors are 3-hexythiophene and alkyl-substituted triphenylamine polymers. One advantage of these devices compared to other chemical sensors is that they can be fabricated through the same technologies that are developed for the fabrication of other organic electronic devices. This can help their mass production, their cheap fabrication, and their miniaturization [99, 100].

3.1 Chemical sensors based on electrostatically charged selective layers

CHEMFETs have many advantages such as the possibility to scale down their size or use current semiconductor fabrication technology for their mass production while maintaining uniform quality across devices [6]. The main difference between chemiresistive sensors and CHEMFETs is the absence of the dielectric layer and gate electrode. This makes chemiresistive sensors simple, inexpensive, and allows for easy incorporation of carbon nanotubes, graphene, and other 2D materials in these sensors. It has been recently reported that the electrostatic gating of semiconducting materials such as CNTs through chemical surface adsorbates can be used to create CHEMFETs without the need for a dielectric layer and a gate electrode [7]. The architecture of the reported sensor is similar to chemiresistive sensors but the function and the response of the sensor is similar to CHEMFETs. It has been shown that the increase in the functional density of the negatively charged adsorbed receptors on CNTs can modulate the charge transport in the tube (charge transport layer). Based on this observation, it was concluded that the sensing mechanism of the device is based on chemically driven electrostatic gating. Therefore, the field effect created through electrostatic gating is similar to the effect of the gate voltage in FETs (CHEMFETs) [7].

Based on the same principle, it has been shown that redox-active oligoanilines such as a phenyl-capped aniline tetramer (PCAT) adsorbed on the surface of a pencil drawn film can be used for the sensing of oxidizing agents in drinking water such as free chlorine [101]. Although a bare pencil film can also be used for the detection of the oxidizing agents in drinking water, the adsorbed PCAT film not only increases the sensitivity of the device but also makes it more selective to free chlorine [102]. The sensing mechanism in this system has been attributed to the temporary protonic doping of PCAT during its oxidation by free chlorine [101]. The protonically doped PCAT will impose an electric field onto the underlying thin pencil drawn substrate and can affect the charge transport in this conductive channel. Another advantage of using a redox-active small molecule as a receptor is the possibility of its chemical or electrochemical reduction after each measurement, which creates the possibility to reset the sensor for continuous sampling [62, 67].

Charge transfer doping at interfaces is another principle which can be used for sensing applications. This chemical doping method is based on the idea that the adsorption of electron donating or electron withdrawing molecules or atoms on surfaces can cause doping of the substrate and change its electronic characteristics such as electrical conductivity. The effectiveness of the doping process between a surface and an adsorbate can be assessed by comparison between the Fermi level of a surface and the electrochemical potential of an adsorbate molecule. Electrons can be added to a surface once the electrochemical potential of a molecule is higher than the Fermi level of the surface. On the other hand, electrons can be removed from a surface if the electrochemical potential of a molecule is lower than the Fermi level of the surface [103].

PCAT (or PANI) is also able to perform charge transfer doping with some surfaces (e. g. iron oxide [104]) and nanomaterials (e. g. SWCNTs [67]). In the former case, it has been shown that the fully reduced PCAT will be oxidized on the surface of an iron oxide thin film while the fully oxidized PCAT will be reduced on the same surface [104]. Based on this idea, a chemical sensor can be constructed. While iron oxides, due to their poor conductivity and instability under ambient conditions, are poor choices for application in chemical sensors [105],

SWCNTs are highly conductive and chemically inert [106]. In addition, nanomaterials are desirable choices for chemical sensing as their high surface to bulk ratio maximizes their interactions with the analyte [39].

It has been shown that the adsorption of PCAT on SWCNTs drop cast between two gold electrodes fabricated on a glass substrate can be used for sensing of free chlorine in drinking water [62]. This ensemble of PCAT-SWCNT can be incorporated into a microfluidic channel which directs the analyte solution to this film. Introduction of aqueous free chlorine to the fully reduced PCAT-SWCNT causes the oxidation of PCAT which leads to p-doping of the SWCNTs and a drop in their electrical resistance [67]. Therefore, the magnitude of the change in the electrical resistance of the system can be related to the concentration of the free chlorine present in the drinking water [62]. It has been argued that percolation networks formed from disordered nanostructures are the most promising architecture for chemical sensing, because such structures will integrate the response of all network elements in the ensemble. Thus, microscopic scale variations between different elements are averaged out leading to a homogenous and reproducible system [107].

4 Conclusion

In this review, the typical transduction mechanisms in chemical sensors were introduced. The working principle of different variations of chemiresistive sensors was described and the most common materials used in each one were mentioned. The advantages and disadvantages of each architecture were discussed. The CHEMFET and its most common configurations were briefly introduced. In addition, we discussed recent work on gateless chemical sensors in which changes in the charge or electron affinity of a molecular layer directly incorporated onto – but distinct from – the conductive film lead to the sensing response. This geometry has several advantages over traditional CHEMFETs such as no need for a gate electrode and dielectric layer.

Funding

The National Science and Engineering Research Council of Canada provided financial support through the Discovery Grant program.

References

[1] Wencel D, Abel T, McDonagh C. Optical chemical pH sensors. Anal Chem. 2014;86:15–29.
[2] Rahman MA, Kumar P, Park DS, Shim YB. Electrochemical sensors based on organic conjugated polymer. Sens. 2008;8:118–41.
[3] Compton RG, Banks CE. Understanding voltammetry. Singapore: World Scientific; 2007.
[4] Seymour EH, Lawrence NS, Compton RG. Reaction with N,N-Diethyl-P-Phenylenediamine: A procedure for the sensitive square-wave voltammetric detection of chlorine. Electroanal. 2003;15:689–94.
[5] Janata J, Josowicz M. Conducting polymers in electronic chemical sensors. Nat Mater. 2003;2:19–24.
[6] Janata J. Thirty years of CHEMFETs - A personal view. Electroanal. 2004;16:1831–35.
[7] Ng AL, Chen C, Kwon H, Peng Z, Lee CS, Wang Y. Chemical gating of a synthetic tube-in-a-tube semiconductor. J Am Chem Soc. 2017;139:3045–51.
[8] Palin AT. The determination of free and combined chlorine in water by the use of Diethyl-P-Phenylene diamine. J Am Water Works Assoc. 1957;49:873–80.
[9] Moberg L, Karlberg B. An Improved N,N′-Diethyl-P-Phenylenediamine (DPD) method for the determination of free chlorine based on multiple wavelength detection. Anal Chim Acta. 2000;407:127–33.
[10] Tang Y, Su Y, Yang N, Zhang L, Lv Y. Carbon nitride quantum dots: A novel chemiluminescence system for selective detection of free chlorine in water. Anal Chem. 2014;86:4528–35.
[11] Jensen JN, Johnson JD. Specificity of the DPD and amperometric titration methods for free available chlorine: A review. J Am Water Works Assoc. 1989;81:59–64.
[12] Rahimi R, Ochoa M, Tamayol A, Khalili S, Khademhosseini A, Ziaie B. A highly stretchable potentiometric pH sensor fabricated via direct laser-writing/machining of carbon-polyaniline composite. ACS Appl Mater Interfaces. 2017;9:9015–23.
[13] Zhao D, Guo X, Wang T, Alvarez NT, Shanov VN, Heineman WR. Simultaneous detection of heavy metals by anodic stripping voltammetry using carbon nanotube thread. Electroanal. 2014;26:488–96.
[14] Jiang G, Goledzinowski M, Comeau FJE, Zarrin H, Lui G, Lenos J, et al. Free-standing functionalized graphene oxide solid electrolytes in electrochemical gas sensors. Adv Funct Mater. 2016;26:1729–36.
[15] Janata J, Josowicz M. Chemical modulation of work function as a transduction mechanism for chemical sensors. Acc Chem Res. 1998;31:241–48.
[16] Seiyama T, Fujiishi K, Nagatani M, Kato A. A new detector for gaseous components using zinc oxide thin films. J Soc Chem Ind Japan. 1963;66:652–55.

[17] Albert KJ, Lewis NS, Schauer CL, Sotzing AG, Stitzel SE, Vaid TP, et al. Cross-reactive chemical sensor arrays. Chem Rev. 2000;100:2595–626.
[18] Göpel W, Schierbaum KD. SnO_2 sensors: current status and future prospects. Sens Actuat B Chem. 1995;26:1–12.
[19] Lange U, Roznyatovskaya NV, Mirsky VM. Conducting polymers in chemical sensors and arrays. Anal Chim Acta. 2008;614:1–26.
[20] Balouria V, Samanta S, Singh A, Debnath AK, Mahajan A, Bedi RK, et al. Chemiresistive gas sensing properties of nanocrystalline Co_3O_4 thin films. Sens Actuators B Chem. 2013;176:38–45.
[21] Korotcenkov G, Brinzari V, Stetter JR, Blinov I, Blaja V. The nature of processes controlling the kinetics of indium oxide-based thin film gas sensor response. Sens Actuators B Chem. 2007;128:51–63.
[22] Song E, Choi JW. Conducting polyaniline nanowire and its applications in chemiresistive sensing. Nanomater. 2013;3:498–523.
[23] Joshi N, Saxena V, Singh A, Koiry SP, Debnath AK, Chehimi MM, et al. Flexible H_2S sensor based on gold modified polycarbazole films. Sens Actuators B Chem. 2014;200:227–34.
[24] Yang L, Li M, Qu Y, Dong Z, Li WJ. Carbon nanotube-sensor-integrated microfluidic platform for real-time chemical concentration detection. Electrophoresis. 2009;30:3198–205.
[25] Robinson JT, Perkins FK, Snow ES, Wei Z, Sheehan PE. Reduced graphene oxide molecular sensors. Nano Lett. 2008;8:3137–40.
[26] Yamazoe N, Miura N. Environmental gas sensing. Sens Actuat B Chem. 1994;20:95–102.
[27] Sun GJ, Lee JK, Choi S, Lee WI, Kim HW, Lee C. Selective oxidizing gas sensing and dominant sensing mechanism of *n*-CaO-Decorated *n*-ZnO nanorod sensors. ACS Appl Mater Interfaces. 2017;9:9975–85.
[28] Adhyapak PV, Mulik UP, Amalnerkar DP, Mulla IS. Low temperature synthesis of needle-like alpha-FeOOH and their conversion into alpha-Fe_2O_3 nanorods for humidity sensing application. J Am Ceram Soc. 2013;96:731–35.
[29] Zappa D, Bertuna A, Comini E, Kaur N, Poli N, Sberveglieri V, et al. Metal oxide nanostructures: preparation, characterization and functional applications as chemical sensors. Beilstein J Nanotechnol. 2017;8:1205–17.
[30] Lin HJ, Gao H, Gao PX. UV-enhanced CO sensing using Ga_2O_3-based nanorod arrays at elevated temperature. Appl Phys Lett. 2017;110:043101.
[31] Song Z, Wei Z, Wang B, Luo Z, Xu S, Zhang W, et al. Sensitive room-temperature H_2S gas sensors employing SnO_2 quantum wire/reduced graphene oxide nanocomposites. Chem Mater. 2016;28:1205–12.
[32] Kim DH, Shim YS, Jeon JM, Jeong HY, Park SS, Kim YW, et al. Vertically ordered hematite nanotube array as an ultrasensitive and rapid response acetone sensor. ACS Appl Mater Interfaces. 2014;6:14779–84.
[33] Jaisutti R, Lee M, Kim J, Choi S, Ha TJ, Kim J, et al. Ultrasensitive room-temperature operable gas sensors using p-type Na: ZnO Nanoflowers for diabetes detection. ACS Appl Mater Interfaces. 2017;9:8796–804.
[34] Cho B, Hahm MG, Choi M, Yoon J, Kim AR, Lee YJ, et al. Charge-transfer-based gas sensing using atomic-layer MoS_2. Sci Rep. 2015;5:8052.
[35] Hazra A, Dutta K, Bhowmik B, Chattopadhyay PP, Bhattacharyya P. Room temperature alcohol sensing by oxygen vacancy controlled TiO_2 nanotube array. Appl Phys Lett. 2014;105:081604.
[36] Xu C, Tamaki J, Miura N, Yamazoe N. Grain size effects on gas sensitivity of porous SnO2-based elements. Sens Actuat B Chem. 1991;3:147–55.
[37] Singh S, Greiner MT, Kruse P. Robust inorganic membranes from detachable ultra-thin tantalum oxide films. Nano Lett. 2007;7:2676–83.
[38] Singh S, Festin M, Barden WRT, Xi L, Francis JT, Kruse P. Universal method for the fabrication of detachable ultrathin films of several transition metal oxides. ACS Nano. 2008;2:2363–73.
[39] Imbault A, Wang Y, Kruse P, Strelcov E, Comini E, Sberveglieri G, et al. Ultrathin gas permeable oxide membranes for chemical sensing: nanoporous Ta_2O_5 test study. Materials. 2015;8:6677–84.
[40] Roy S, Raju R, Chuang HF, Cruden BA, Meyyappan M. Modeling gas flow through microchannels and nanopores. J Appl Phys. 2003;93:4870–79.
[41] Lange U, Mirsky VM. Chemiresistors based on conducting polymers: A review on measurement techniques. Anal Chim Acta. 2011;687:105–13.
[42] Fowler JD, Virji S, Kaner RB, Weiller BH. Hydrogen detection by polyaniline nanofibers on gold and platinum electrodes. J Phys Chem C. 2009;113:6444–49.
[43] Liu C, Noda Z, Sasaki K, Hayashi K. Development of a polyaniline nanofiber-based carbon monoxide sensor for hydrogen fuel cell application. Int J Hydrog Energy. 2012;37:13529–35.
[44] Zeng FW, Liu XX, Diamond D, Lau KT. Humidity sensors based on polyaniline nanofibres. Sens Actuators B Chem. 2010;143:530–34.
[45] Song E, Choi JW. Self-calibration of a polyaniline nanowire-based chemiresistive pH sensor. Microelectr Eng. 2014;116:26–32.
[46] Charlesworth JM, Partridge AC, Garrard N. Mechanistic Studies on the interactions between poly(pyrrole) and organic vapors. J Phys Chem. 1993;97:5418–23.
[47] Wang F, Yang Y, Swager TM. Molecular recognition for high selectivity in carbon nanotube/polythiophene chemiresistors. Angew Chem Int Ed. 2008;47:8394–96.
[48] Gruber J, Yoshikawa EKC, Bao Y, Geise HJ. Synthesis of a novel poly(p-Phenylene-Vinylene) derivative and its application in chemiresistive sensors for electronic noses with an unusual response to organic vapours. e-Polym. 2004;4:014.
[49] Tanese MC, Torsi L, Cioffi N, Zotti LA, Colangiuli D, Farinola GM, et al. Poly(phenyleneethynylene) polymers bearing glucose substituents as promising active layers in enantioselective chemiresistors. Sens Actuators B Chem. 2004;100:17–21.
[50] Huang J, Virji S, Weiller BH, Kaner RB. Polyaniline nanofibers: facile synthesis and chemical sensors. J Am Chem Soc. 2003;125:314–15.
[51] Xue M, Li F, Chen D, Yang Z, Wang X, Ji J. High-oriented polypyrrole nanotubes for next-generation gas sensor. Adv Mater. 2016;28:8265–70.
[52] Virji S, Huang JX, Kaner RB, Weiller BH. Polyaniline nanofiber gas sensors: examination of response mechanisms. Nano Lett. 2004;227:104–104.
[53] Virji S, Kaner RB, Weiller BH. Hydrogen sensors based on conductivity changes in polyaniline nanofibers. J Phys Chem B. 2006;110:22266–70.
[54] Meyyappan M. Carbon nanotube-based chemical sensors. Small. 2016;12:2118–29.

[55] Llobet E. Gas sensors using carbon nanomaterials: A review. Sens Actuators B Chem. 2013;179:32–45.
[56] Schedin F, Geim AK, Morozov SV, Hill EW, Blake P, Katsnelson MI, et al. Detection of individual gas molecules adsorbed on graphene. Nat Mater. 2007;6:652–55.
[57] Varghese SS, Varghese SH, Swaminathan S, Singh KK, Mittal V. Two-dimensional materials for sensing: graphene and beyond. Electronics. 2015;4:651–87.
[58] Kurra N, Kulkarni GU. Pencil-on-paper: electronic devices. Lab Chip. 2013;13:2866–73.
[59] Wakeland S, Martinez R, Grey JK, Luhrs CC. Production of graphene from graphite oxide using urea as expansion-reduction agent. Carbon. 2010;48:3463–70.
[60] Bianco GV, Losurdo M, Giangregorio MM, Capezzuto P, Bruno G. Exploring and rationalizing effective N-doping of large area CVD-graphene by NH_3. Phys Chem Chem Phys. 2014;16:3632–39.
[61] Qin Y, Kwon HJ, Subrahmanyam A, Howlader MMR, Selvaganapathy PR, Adronov A, et al. Inkjet-printed bifunctional carbon nanotubes for pH sensing. Mater Lett. 2016;176:68–70.
[62] Hsu LHH, Hoque E, Kruse P, Selvaganapathy PR, A Carbon nanotube based resettable sensor for measuring free chlorine in drinking water. Appl Phys Lett. 2015;106:63102.
[63] Hong S, Myung S. Nanotube electronics: A flexible approach to mobility. Nat Nanotechnol. 2007;2:207–08.
[64] Singh S, Kruse P. Carbon nanotube surface science. Int J Nanotechnol. 2008;5:900–29.
[65] Moonoosawmy KR, Kruse P. Cause and consequence of carbon nanotube doping in water and aqueous media. J Am Chem Soc. 2010;132:1572–77.
[66] Moonoosawmy KR, Kruse P. To dope or not to dope: the effect of sonicating single-wall carbon nanotubes in common laboratory solvents on their electronic structure. J Am Chem Soc. 2009;130:13417–24.
[67] Klinke C, Chen J, Afzali A, Avouris P. Charge transfer induced polarity switching in carbon nanotube transistors. Nano Lett. 2005;5:555–58.
[68] Li J, Lu Y, Ye QL, Han J, Meyyappan M. Carbon nanotube based chemical sensors for gas and vapor detection. Nano Lett. 2003;3:929–33.
[69] Arnold MS, Green AA, Hulvat JF, Stupp SI, Hersam MC. Sorting carbon nanotubes by electronic structure using density differentiation. Nat Nanotechnol. 2006;1:60.
[70] Cao Q, Han S, Tersoff J, Franklin AD, Zhu Y, Zhang Z. End-bonded contacts for carbon nanotube transistors with low, size-independent resistance. Science. 2015;350:68–71.
[71] Geim AK, Novoselov KS. The rise of graphene. Nat Mater. 2007;6:183–91.
[72] McCurle JW. Diamagnetism of graphite. Phys Rev. 1956;104:666–71.
[73] Slonczewski JC, Weiss PR. Band structure of graphite. Phys Rev. 1958;330:272–79.
[74] Wallace PR. The band theory of graphite. Phys Rev. 1947;71:622–34.
[75] Mermin ND. Crystalline order in two dimensions. Phys Rev. 1968;176:250–54.
[76] Novoselov KS, Geim AK, Morozov SV, Jiang D, Zhang Y, Dubonos SV, et al. Electric field effect in atomically thin carbon films. Science. 2004;306:666–69.
[77] Levendorf MP, Ruiz-Vargas CS, Garg S, Park J. Transfer-free batch fabrication of single layer graphene transistors. Nano Lett. 2009;9:4479–83.
[78] Geim AK. Graphene: status and prospects. Science. 2009;324:1530–34.
[79] Allen MJ, Tung VC, Kaner RB. Honeycomb carbon: A review of graphene. Chem Rev. 2010;110:132–45.
[80] Denis PA, Iribarne F. Comparative Study of defect reactivity in graphene. J Phys Chem C. 2013;117:19048–55.
[81] Guo B, Fang L, Zhang B, Gong JR. Graphene doping: A review. Insciences J. 2011;1:80–89.
[82] Partoens B, Peeters F. From graphene to graphite: electronic structure around the K point. Phys Rev B. 2006;74:75404.
[83] Liu J, Liu Z, Barrow CJ, Yang W. Molecularly engineered graphene surfaces for sensing applications: A review. Anal Chim Acta. 2015;859:1–19.
[84] Rutter GM, Crain JN, Guisinger NP, Li T, First PN, Stroscio JA. Scattering and interference in epitaxial graphene. Science. 2007;317:219–22.
[85] Varghese SS, Lonkar S, Singh KK, Swaminathan S, Abdala A. Recent advances in graphene based gas sensors. Sens Actuat B Chem. 2015;218:160–83.
[86] Ang PK, Chen W, Thye A, Wee S, Loh KP. Solution-gated epitaxial graphene as pH sensor solution-gated epitaxial graphene as pH sensor. J Am Chem Soc. 2008;130:14392–93.
[87] Shirsat MD, Sarkar T, Kakoullis J, Jr., Myung NV, Konnanath B, Spanias A, et al. Porphyrine-functionalized single-walled carbon nanotube chemiresistive sensor arrays for VOCs. J Phys Chem C. 2012;116:3845–50.
[88] Liu SF, Moh LCH, Swager TM. Single-walled carbon nanotube—metalloporphyrin chemiresistive gas sensor arrays for volatile organic compounds. Chem Mater. 2015;27:3560–63.
[89] Rushi A, Datta K, Ghosh P, Mulchandani A. Selective discrimination among benzene, toluene, and xylene: probing metalloporphyrin-functionalized single-walled carbon nanotube-based field effect transistors. J Phys Chem C. 2014;118:24034–41.
[90] Zhao J, Hashmi A, Xu J, Xue W. A compact lab-on-a-chip nanosensor for glycerol detection. Appl Phys Lett. 2012;100:243109.
[91] Gautam M, Jayatissa AH. Ammonia gas sensing behavior of graphene surface decorated with gold nanoparticles. Solid State Electron. 2012;78:159–65.
[92] Yavari F, Castillo E, Gullapalli H, Ajayan PM, Koratkar N. High sensitivity detection of NO_2 and NH_3 in air using chemical vapor deposition grown graphene. Appl Phys Lett. 2012;100:203120.
[93] Meng H, Yang W, Ding K, Feng L, Guan Y. Cu_2O nanorods modified by reduced graphene oxide for NH_3 sensing at room temperature. J Mater Chem A. 2015;3:1174–81.
[94] Ye Z, Jiang Y, Tai H, Yuan Z. The investigation of reduced graphene oxide/P3HT composite films for ammonia detection. Integr Ferroelectr. 2014;154:73–81.
[95] Dua V, Surwade SP, Ammu S, Agnihotra SR, Jain S, Roberts KE, et al. All-organic vapor sensor using inkjet-printed reduced graphene oxide. Angew Chem Int Ed. 2010;49:2154–57.

[96] Qin Y, Kwon HJ, Howlader MMR, Deen MJ. Microfabricated electrochemical pH and free chlorine sensors for water quality monitoring: recent advances and research challenges. RSC Adv. 2015;5:69086–109.
[97] Zhang T, Petelenz D, Janata J. Temperature-controlled kelvin microprobe. Sens Actuat B Chem. 1993;12:175–80.
[98] Li J, Petelenz D, Janata J. Suspended gate field-effect transistor sensitive to gaseous hydrogen cyanide. Electroanal. 1993;5:791–94.
[99] Torsi L, Magliulo M, Manoli K, Palazzo G. Organic field-effect transistor sensors: A tutorial review. Chem Soc Rev. 2013;42:8612–28.
[100] Zhang C, Chen P, Hu W. Organic field-effect transistor-based gas sensors. Chem Soc Rev. 2015;44:2087–207.
[101] Mohtasebi A, Broomfield AD, Chowdhury T, Selvaganapathy PR, Kruse P. Reagent-free quantification of aqueous free chlorine via electrical readout of colorimetrically functionalized pencil lines. ACS Appl Mater Interfaces. 2017;9:20748–61.
[102] Hoque E, Hsu LHH, Aryasomayajula A, Selvaganapathy PR, Kruse P. Pencil-drawn chemiresistive sensor for free chlorine in water. IEEE Sens Lett. 2017;1:4500504.
[103] Kim KK, Kim SM, Lee YH. Chemically conjugated carbon nanotubes and graphene for carrier modulation. Acc Chem Res. 2016;49:390–99.
[104] Mohtasebi A, Chowdhury T, Hsu LHH, Biesinger MC, Kruse P. Interfacial charge transfer between phenyl- capped aniline tetramer films and iron oxide surfaces. J Phys Chem C. 2016;120:29248–63.
[105] Xue M, Wang S, Wu K, Guo J, Guo Q. Surface structural evolution in iron oxide thin films. Langmuir. 2011;27:11–14.
[106] Dresselhaus MS, Jorio A, Saito R. Characterizing graphene, graphite, and carbon nanotubes by raman spectroscopy. Annu Rev Condens Matter Phys. 2010;1:89–108.
[107] Snow AW, Perkins FK, Ancona MG, Robinson JT, Snow ES, Foos EE. Disordered nanomaterials for chemielectric vapor sensing: A review. IEEE Sens J. 2015;15:1301–20.